[11]E. Vogt, Rev. Mod. Phys. 34, 723 (1962).
[12]R. G. Thomas, Phys. Rev. 97, 224 (1955).
[13]F. R. Gantmacher, *Matrix Theory* (Chelsea Pub. Co., New York, 1960).
[14]As the form of the transition matrix T (or of U) is of the same type as the one introduced by R. L. Kapur and R. Peierls [Proc. Roy. Soc. (London) A166, 277 (1938)] for the case of one-body resonances, it has become customary to follow the terminology of Lane and Thomas (Ref. 3) and to refer to this approach as to a "generalized Kapur-Peierls formalism."
[15] F. T. Adler and D. B. Adler, USAEC Report Nos. CONF-660303 and COO-2022-4 (unpublished).
[16]D. B. Adler and F. T. Adler, USAEC Report No. ANL-6792 (unpublished); F. T. Adler and D. B. Adler, Trans. Am. Nucl. Soc. 5, 53 (1962); 5, 407 (1962); in *Proceedings of the Conference on Neutron Cross Section Technology*, Natl. Bur. Std. Special Publication No. 299, edited by D. T. Goldman (U.S. GPO, Washington, D. C., 1968), Vol. II, p. 967.
[17]If the energy dependence of the poles and residues of the collision matrix is fully negligible, the multilevel expansions of Eqs. (10) and (11) appear in form equivalent to those of J. Humblet and L. Rosenfeld [Nucl. Phys. 26, 529 (1971), and 22, 594 (1961)] and J. Humblet, in *Fundamentals of Nuclear Theory*, edited by A. de-Shalit and C. Villi (International Atomic Energy Agency, Vienna, 1967), Chap. 7. The approach used in this paper differs from the one of Rosenfeld-Humblet in its explicit relation to the R-matrix theory.
[18]F. T. Adler and D. B. Adler, in *Proceedings of the Second International Conference on Nuclear Data for Reactors, Helinski, June 1970* (International Atomic Energy Agency, Vienna, 1970), Vol. 2., pp. 777–788.
[19]D. B. Adler, U. S. AEC Report Nos. COO-2022-5, 1970 and COO-1564-4, 1967 (unpublished).
[20]D. B. Adler and F. T. Adler, Trans. Am. Nucl. Soc. 14, 2, 803 (1971), and Bull. Am. Phys. Soc., Tucson Meeting, November 1971.
[21]D. B. Adler and F. T. Adler, U. S. AEC Report No. COO-1546-7, 1968 (unpublished).
[22]J. D. Garrison, Ann. Phys. (N.Y.) 50, 355 (1968).
[23]D. R. Harris, U. S. AEC Report No. LA 4327, 1970 (unpublished), and Trans. Am. Nucl. Soc. 8, 216 (1965).

PHYSICAL REVIEW C VOLUME 6, NUMBER 3 SEPTEMBER 1972

Spectroscopy of ^{101}Mo by Sub-Coulomb Stripping*

W. L. Sievers, D. A. Close, C. J. Umbarger,† R. C. Bearse, and F. W. Prosser, Jr.
Department of Physics, University of Kansas, Lawrence, Kansas 66044
(Received 7 April 1972)

Sub-Coulomb stripping has been employed to study ^{101}Mo with 3.75-MeV deuterons. Proton groups assigned to states in ^{101}Mo at excitation energies of 0, 57, 239, 290, 349, 480, 540, 561, 812, 851, and 898 keV were observed. The states at 349, 561, and 851 keV have not been reported previously. The ground state and the excited state at 349 keV have been shown to be $\frac{1}{2}^+$ states with spectroscopic factors of 0.42 and 0.16. Tentative assignments of $l_n=2$ have been made for the states at 57, 239, 290, and 480 keV. Assuming a $\frac{3}{2}^+$ nature for these states, the spectroscopic factors are 0.25, 0.09, 0.12, and 0.11, respectively. The sum of the spectroscopic factors for $l=0$ and $l=2$ transitions are shown to be consistent with previous results from stripping and pickup reactions on neighboring nuclei.

I. INTRODUCTION

Very little information is available about the nucleus ^{101}Mo. Most of the information on the neutron single-particle properties of ^{101}Mo states is the result of an early study by Hjorth and Cohen,[1] who used the (d, p) reaction to study ^{101}Mo. They reported that the three highest energy proton groups in their spectra which result from states through 530 keV in excitation energy, each contained at least two states; one of these groups was later found to contain three states. In addition there were strong contaminant groups present.

Recently Booth *et al.*[2] investigated a number of zirconium and molybdenum nuclides seeking to show that many of the states for which $g_{7/2}$ assignments had been made actually had $l_n=5$ and should be assigned to the $1h_{11/2}$ orbital. It was found that in ^{101}Mo, instead of a doublet at excitation energies of 0.26 and 0.31 MeV, there were three states within a range of 45 keV. The lowest of these was reported to have $l_n=4$; the middle state was at 0.276 MeV and had $l_n=5$ and a spectroscopic factor of 0.44. No other information concerning ^{101}Mo was given.

The other information available about ^{101}Mo is from a study of analog resonances in the ^{100}Mo-(p, p') reaction by Moore *et al.*[3]

The theory of sub-Coulomb stripping, which has been employed in this study, has been developed and refined by several authors,[4–12] and several experimental investigations[13–20] have been made utilizing this technique. The greater accuracy with which spectroscopic factors can be determined re-

sults from the fact that nuclear contributions are mostly eliminated from the deuteron-target and proton-recoil nucleus interactions. Thus the nuclear potential is important only for the transferred neutron.

The chief disadvantage of sub-Coulomb stripping is the low cross section. As a result, small quantities of low-mass contaminants can make large contributions to the experimental spectra.

In this study the yields of proton groups and their dependence on detector angle and bombarding energy were utilized to extract spectroscopic factors and values of the orbital angular momentum of the transferred neutrons.

II. EXPERIMENTAL METHOD

A. Targets

The two targets used in this study were self-supporting molybdenum foils. A target foil, enriched to 97.42% in ^{100}Mo, was prepared by a commercial firm.[21] This foil was attached to the target frame with a lacquer. For a natural abundance target an electron beam deposition gun was used to evaporate molybdenum onto a glass slide which was covered with a layer of NaCl from a previous evaporation. The molybdenum was floated off the slide in distilled water and picked up with a target frame in the usual fashion. After drying, lacquer was used to insure that the foil was securely attached to the frame.

The enriched target had an areal density of 206 μg/cm^2 which corresponds to a 14-keV energy loss by 3.75-MeV deuterons and a 6.6-keV loss by 6.5-MeV protons. The natural target had an areal density of approximately 66 μg/cm^2. This target was used to identify proton groups from other isotopes of Mo; the enriched target was used for all other data reported here.

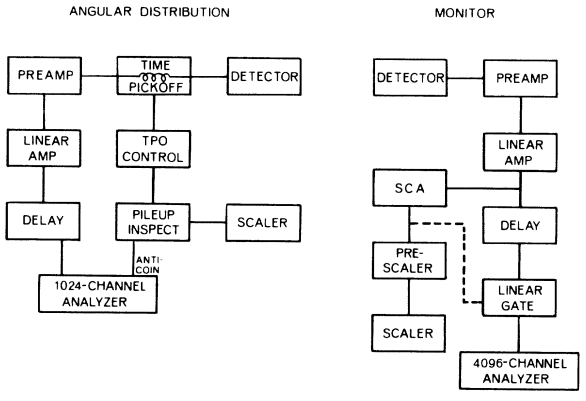

FIG. 1. Block diagram of the electronics. The linear gate and multichannel analyzer portion of the monitor circuit were used only to determine that the single-channel analyzer window was accurately centered over the elastic group.

B. Beam and Scattering Chamber

The experiments were performed using deuterons from the University of Kansas Van de Graaff accelerator. For the measurement of excitation functions, beams were used with currents of approximately 0.7 μA and energies between 3.0 and 3.8 MeV. For those of angular distributions, the currents were approximately 0.2 μA and the deuteron energy was 3.75 MeV.

The 12-in. scattering chamber previously described[22,23] was employed. The protons were detected by a 50-mm^2 silicon surface-barrier detector with a depletion depth of 500 μ. A collimator in front of the detector had two rectangular apertures. The first aperture was 6.6 cm from the target center, and defined a solid angle of 1.46×10^{-3} sr, with a half-angle of 0.0138 rad, or 0.79° in the horizontal direction. The second aperture was positioned to reduce the possibility of particles scattered from the edges of the first aperture reaching the detector. A Teflon ring between the detector and the collimator cartridge insured that particles could not reach the detector surface except through the apertures, and a small horseshoe magnet was placed in front of the collimator to deflect electrons produced at the target.

The data for the excitation curve were taken with the target oriented at a 45° angle from the beam direction. For the angular distribution, the target was oriented so that its normal direction was 30° from the beam direction. A 25-mm^2 detector was used as a monitor and was located in the wall of the chamber at 150° for the angular distribution and at 110° for the excitation function.

C. Electronics

Figure 1 is a block diagram of the electronics. Since the close spacing of the levels required optimal resolution, foils could not be used to stop the elastic deuterons. These deuterons caused high counting rates, up to 8000 sec^{-1} at forward angles in the angular distribution measurements and at the higher currents used for the excitation functions. Hence pileup rejection was necessary to maintain adequate resolution. As indicated in Fig. 1, this was accomplished by the use of a pileup inspector module. Two pulses occurring in the time range from about 0.02 to 2 μsec caused the generation of a pulse which activated the anticoincidence gate of the multichannel analyzer. (The lower limit is that given by the manufacturer, but was consistent with the counting rate observed in the double energy elastic peak in the spectra.) Bi-

polar active filter pulse shaping was used with a nominal time constant of 0.5 μsec. The multichannel analyzer was set to accept pulses with rise times (from threshold to maximum) of up to 0.8 μsec. At this time, and in the absence of an anticoincidence pulse, a linear gate in the analyzer was closed and remained closed for a fixed time of 13 μsec. The anticoincidence pulse was maintained for 4 μsec, so that double pulses occurring near the end of the analysis of a previous pulse would also be rejected. Thus only pulse pairs which occurred within the minimum rejection time of about 20 nsec would be incorrectly interpreted.

The dead-time calculation for the proton detector was based primarily on the characteristics of the pileup inspector and the multichannel analyzer. This was obtained by multiplying the number of anticoincidence pulses by 2 μsec and the number of analyzed pulses by 13.8 μsec. The overlap of these effects and other second-order corrections were included in the final calculation. Dead-time correction of the monitor detector was based on the experimental determination of the relative observed yield of elastic deuterons for a range of beam currents.

D. Other Experimental Aspects

In the excitation-function spectra the resolution was about 39 keV and dead-time losses were 4 to 5%. In the angular-distribution spectra, the resolution was 28 to 32 keV, depending on angle, and the dead time ranged from 1.7 to 12.6%. The improvement in resolution was due to the decreased beam current and to the change in orientation of the target, which reduced the deuteron and proton energy losses in the target.

The Van de Graaff energy calibration was determined at the 1.69-MeV resonance in the ^{12}C(p, p) reaction. Elastic scattering of 1-MeV protons by molybdenum was observed at $\pm 66^\circ$ and $\pm 72^\circ$ to check the symmetry of the scattering chamber. The yields were fitted to the Rutherford scattering equation and were found to require an angle correction of 1.7°. This error appeared to be caused by a misalignment of the beam collimation system and the indexing of the scattering chamber. In any case, any energy variation of this correction would have only a small effect on the calculated cross sections at the angles used in the present investigation.

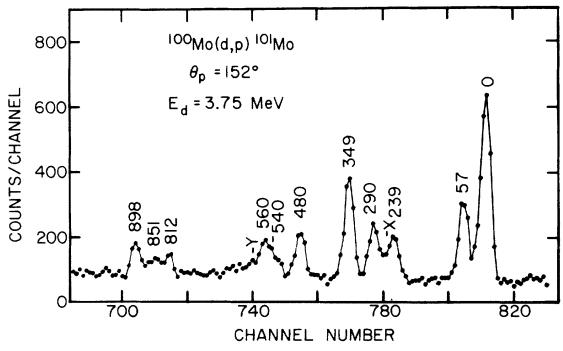

FIG. 2. A portion of the particle spectrum at 152°. The numbers above each peak are the excitation energy (in keV) of the corresponding state in ^{101}Mo. The structure labeled Y is due to the (d, p) reaction on another Mo isotope, probably ^{92}Mo or ^{94}Mo. X denotes a small contribution from a light-element reaction.

III. ANALYSIS

A. Q Value and Energy Levels

Figure 2 illustrates a portion of the spectrum obtained at 152°. The energy scales of the spectra were calibrated with the strong ground-state proton groups from the reactions ^{12}C(d, p)^{13}C and ^{16}O(d, p)^{17}O. The 14 calibration points which were used were from six spectra at angles from 58 to 152° and the corresponding energies ranged from about 4 MeV to about 6 MeV. A linear least-squares-fitting program was used to extract the energies of 10 ^{101}Mo proton groups in each of three spectra, at 88, 122, and 152°. The proton groups from the carbon and oxygen contaminants showed clear components from both sides of the target. The energy average of these components was used in the calibration of the spectra. These energies ranged from about 5.7 to 6.76 MeV. Although 6.76 MeV was beyond the range of available calibration points, tests with a pulser gave an upper limit of 2 keV for the error from nonlinearity of the electronics in the range of 6.0 to 6.76 MeV. These proton energies were compared to the results of relativistic kinematics calculations to obtain an improved Q value for the reaction and accurate excitation energies in ^{101}Mo. All groups ascribed to states in ^{101}Mo varied in energy with angle correctly for a target with $A \simeq 100$ and were appropriately stronger with the enriched target than with the natural molybdenum target. The final values, listed in Table I, are averages of the results from three spectra, at 88, 122, and 152°. The Q value obtained is 3161 ± 6 keV, to be compared with the previous value of 3165.6 ± 19.3 keV.[24]

B. Distorted-Wave Born-Approximation Calculations

Distorted-wave Born-approximation (DWBA) calculations were performed using the program DWUCK.[25,26] The deuteron parameters used were extrapolated from the set obtained by Perey and

Perey.[27] The proton parameters are due to Perey.[28] Spin-orbit potentials were found to give negligible contribution to the cross sections. All optical-model parameters used are given in Table II. The calculations were zero-range calculations with no lower cutoff on the radial integrals, with surface absorption, and with a Woods-Saxon neutron potential well.

The DWBA cross sections, $\sigma_{DW}(\theta)$, are related to the experimental cross section $(d\sigma/d\Omega)$ by

$$\frac{d\sigma}{d\Omega}=1.53\frac{2J_f+1}{2J_i+1}S\frac{2s+1}{2}\frac{\sigma_{DW}(\theta)}{2j+1}.$$

Since, for the ^{100}Mo(d, p) reaction, $J_i=0$, $s=\frac{1}{2}$, and $J_f=j$, this reduces to

$$\frac{d\sigma}{d\Omega}=1.53\,S\sigma_{DW}(\theta), \qquad (1)$$

where the constant 1.53 is a normalization factor based on the Hulthen wave function for the deuteron, and S is the spectroscopic factor.

C. Cross Sections

Yields were extracted by peak-stripping techniques and corrected for differences in dead time, in beam charge collected, and in center-of-mass solid angle. Absolute cross sections were obtained by multiplying the corrected yields by the ratio of elastic deuteron cross sections calculated by DWUCK to similarly corrected experimental elastic deuteron yields. Since the calculated cross sections differed from pure Rutherford scattering values by less than $\frac{1}{2}$%, any errors introduced by using the theoretical cross sections are negligible. Since the deuteron yields were greater than 10^7 counts in all spectra, the statistical error is also negligible. This ratio (of cross section to yield) was also calculated from knowledge of the integrated deuteron flux, the target thickness, the density of atoms in the target, and the solid angle. The two values of the ratio differed by about 10%, within the estimated 12% error of the latter value.

D. Angular Distributions, l_n Values, and Spectroscopic Factors

The angular distributions are shown in Figs. 3 and 4. A number of peaks due to low-Z contaminants, increasing in proton energy relative to ^{101}Mo proton energies as the detection angle decreased, obliterated peaks corresponding to states

TABLE I. Levels in ^{101}Mo obtained in the present study compared to values obtained in Refs. 1 and 2.

Hjorth and Cohen				Booth *et al.*				Present study			
E_x (keV)	l_n	J^π	S	E_x (keV)	l_n	J^π	S	E_x (keV)	l_n	J^π	S
0 [a]	0	$\frac{1}{2}^+$	0.42					0	0	$\frac{1}{2}^+$	0.42
60 [a]	2	$\frac{3}{2}^+$	0.23					57 ± 2	2	$\frac{3}{2}^+$	0.25
260 [a]	(4)	$\frac{7}{2}^+$	0.52	(260)	4	...	...	239 ± 2	2(0, 1)	$(\frac{3}{2}^+)$	0.09
				276	5	$\frac{11}{2}^-$	0.44				
310 [a]	2	$\frac{5}{2}^+$	0.28	(310)	...	...	...	290 ± 2	2(0, 1)	$(\frac{3}{2}^+)$	0.12
								349 ± 2	0	$\frac{1}{2}^+$	0.16
470 [a]	2	$\frac{3}{2}^+$	0.11					480 ± 3	2(1)	$(\frac{3}{2}^+)$	0.11
530 [a]	(1)	$(\frac{3}{2}^-)$	0.13					540 ± 10 [a]	...	...	b
								561 ± 7 [a]	...	...	c
700	(0)	$(\frac{1}{2}^+)$	0.04								
800	(1)	$(\frac{3}{2}^-)$	0.07					812 ± 4	...	...	(0.02 for $l_n=0$)
								851 ± 6	...	...	(0.02 for $l_n=0$)
900	(0)	$(\frac{1}{2}^+)$	0.15					898 ± 3	0, 2(1)	$(\frac{1}{2}^+, \frac{3}{2}^+)$	(0.03, 0.05)
1010	(0)	$(\frac{1}{2}^+)$	0.08								
1100	...	...	...								
1300 [a]	...	...	...								
1420 [a]	...	...	...								

[a] Member of unresolved group.
[b] Strength comparable to that of 480 keV.
[c] Strength of perhaps $\frac{1}{3}$ that at 480 keV.

in ^{101}Mo of higher excitation. However, all ^{101}Mo states up to 1.1 MeV that were significantly populated could be seen at 152°. No transitions were observed to states reported at 0.70 or 1.01 MeV.[1] If either of these states exist, its spectroscopic factor is about 0.01 or less or its orbital angular momentum is 4 or greater. Neither possibility is consistent with the results of previous investigations[1] (see Table I).

The angular distributions calculated for $l_n = 0$, 2, and 4 for the ground-state transition are shown in Fig. 3. Those for other states are similar in shape. The $l_n = 1$ angular distributions have a shape intermediate between the shapes for $l_n = 2$ and 4. The $l_n = 5$ angular distributions are even steeper than those for $l_n = 4$ in the 50 to 180° range. For higher values of l_n the centrifugal contribution to the effective potential barrier is greater; hence the backward peaking, characteristic of sub-Coulomb barrier stripping, is increased and the slopes in the transitions from forward to backward angles in the angular distributions are greater.

Values of l_n were determined by comparing the fits of DWBA angular distributions for various l_n to the experimental angular distributions; the results are shown in Figs. 3 and 4. Spectroscopic factors for each state were calculated by scaling the DWBA angular distribution to fit the experimental cross section. From Eq. (1) the scaling factor

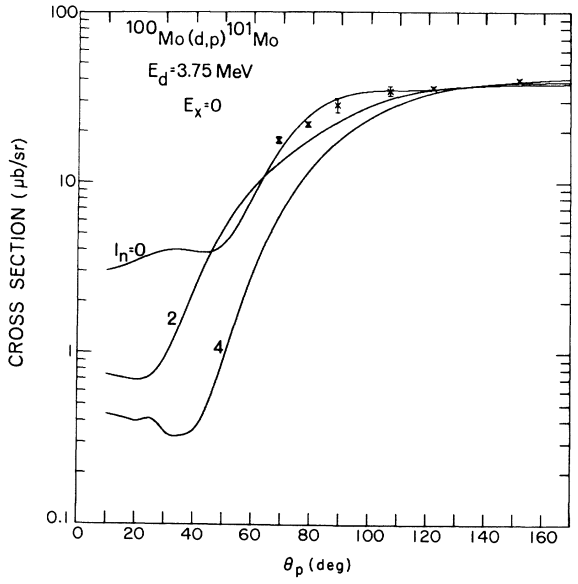

FIG. 3. Angular distribution of the ^{101}Mo ground-state proton group. The solid lines represent the results of DWBA calculations for $l = 0$, 2, and 4. The $l = 0$ theoretical angular distribution has been adjusted vertically to fit the data; the others are normalized to this angular distribution at 135° in order to emphasize the differences in slope in the 70–120° range.

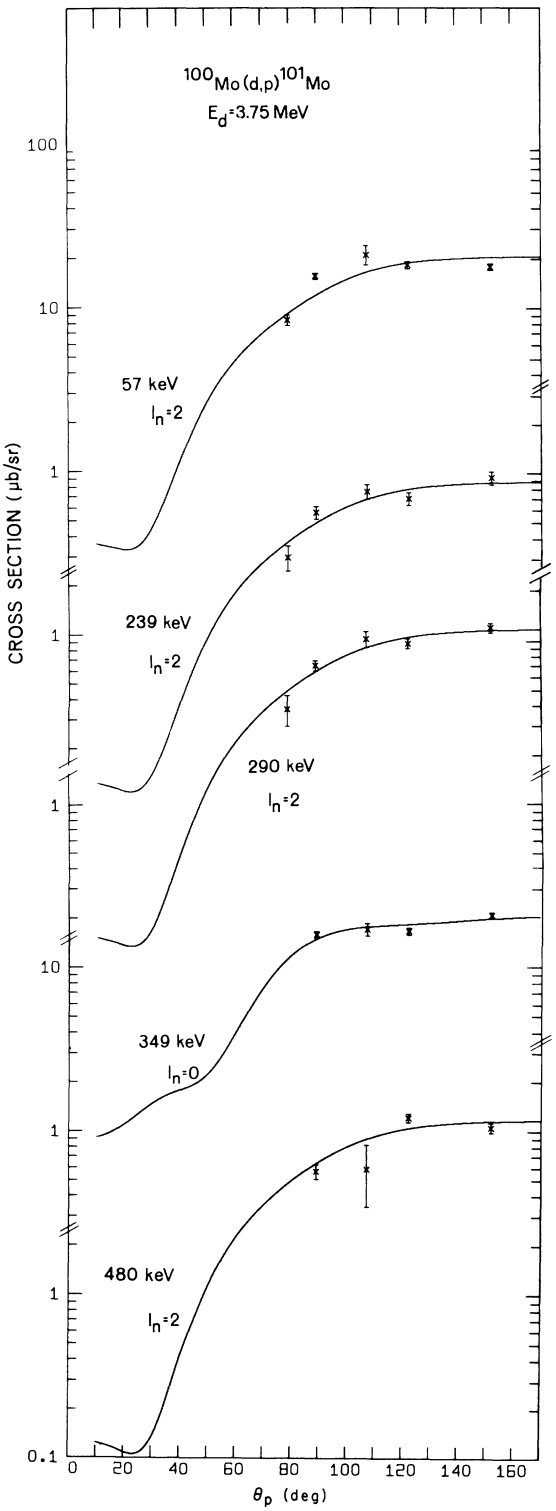

FIG. 4. Angular distributions of proton groups corresponding to excited states of ^{101}Mo. The solid lines are the results of the DWBA calculation for the transferred orbital angular momentum which best fitted the experimental data.

is 1.53S.

Sub-Coulomb stripping cross sections, which increase rapidly with increasing deuteron energy, have greater slopes for larger values of l_n. The slopes from DWBA calculations of the ^{100}Mo(d,p) excitation functions were compared to the experimental slopes. Although the DWBA slopes were consistently slightly low, as is shown for the ground state in Fig. 5, a check of their dependence on W_d and various deuteron and proton radius and diffuseness parameters showed that this consistent deviation could be eliminated by a combination of small arbitrary changes in the optical parameters. However, it was felt that the data did not contain a sufficient number of cases to justify the use of such arbitrary changes. The experimental slopes were not sufficiently accurate to permit their use in making definite l_n assignments. However, the results for the strongest three groups (at 0, 57, and 349 keV) are consistent with the assignments made from the angular distributions.

IV. RESULTS AND DISCUSSION

The results are summarized in Table I and Fig. 6. Single-particle states in the neutron shell above $N=50$ include the $2d_{5/2}$, $1g_{7/2}$, $3s_{1/2}$, $2d_{3/2}$, and $1h_{11/2}$ orbitals. It was assumed that the $d_{5/2}$ subshell is essentially full and spectroscopic factors for d strengths were calculated assuming $j=\frac{3}{2}$. No p or f transitions are expected in nuclei of mass about 100 except at high excitation energies. Therefore p or f admixtures in states populated in the present experiment would be very small, and spectroscopic factors of even a few hundredths are expected to be too large to be realistic. This was the basis for not considering $l=3$ for states at 239, 290, and 480 keV or $l=1$ for states at 0, 57, and 349 keV; in all these cases S would have been greater than 0.13. In addition, the values of S required for $l=1$ (0.04 to 0.05) would be unusually large in this region and, hence, tend to rule out such assignments for states at 239, 290, and 480 keV.

There is excellent agreement with Hjorth and Cohen[1] on l_n and S for the ground state and first excited state. Their failure to observe a state at

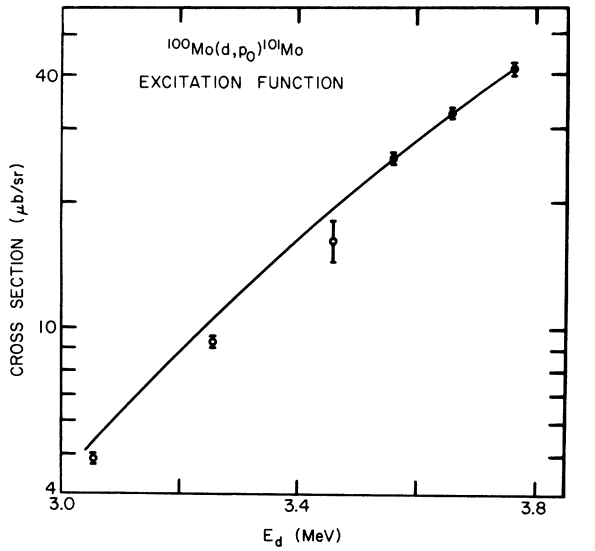

FIG. 5. Excitation function for the ground-state transition. The slope and curvature are typical of the excitation functions for the transitions to other states in ^{101}Mo.

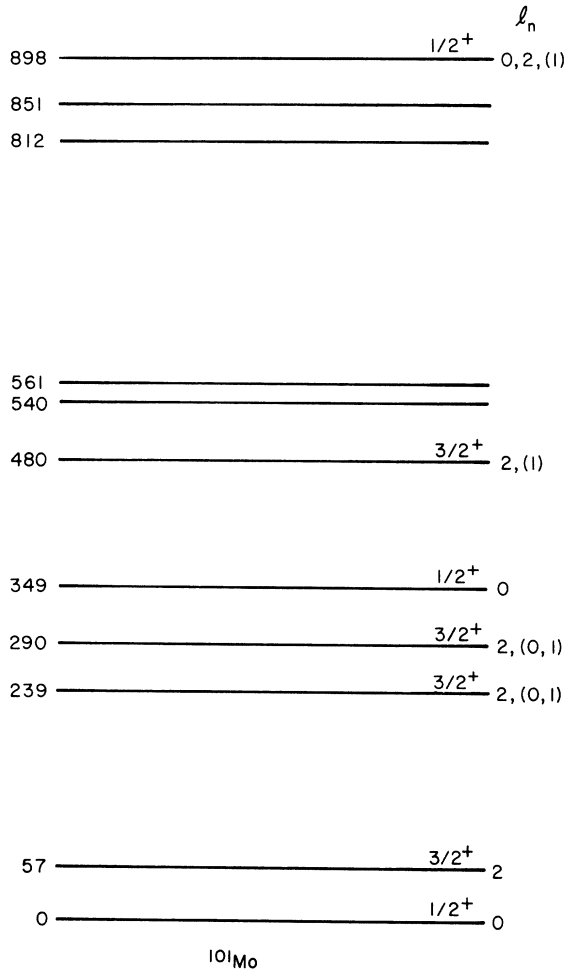

FIG. 6. Energy level diagram for ^{101}Mo, showing levels observed in this experiment. The l_n values in parentheses are those which are significantly less probable but not completely ruled out by the angular distributions. The indicated values of J^π are those assumed in the tabulation of spectroscopic factors. Other assignments commensurate with the l_n values cannot be eliminated.

TABLE II. Optical-model parameters used in the DWBA calculations.

	V (MeV)	$4W$ (MeV)	r_0 (fm)	a (fm)	r'_0 (fm)	a' (fm)	r_{0C} (fm)
d	96	96	1.20	0.69	1.24	0.66	1.25
p	59.5	56	1.25	0.65	1.25	0.47	1.25
n	a	···	1.25	0.65	···	···	···

[a] The neutron well depth was adjusted to give the transferred neutron a binding energy of $Q(d,p)+2.23$ MeV.

about 350 keV is probably due to the location of the ground-state proton group from the reaction ^{12}C-$(d,p)^{13}$C at the extreme forward angles where the cross section for the $l=0$ transfer in ^{101}Mo would be high. The state they observed at 0.31 MeV with $l_n=2$ is probably the state located at 290 keV in the present experiment.

Eidens, Roeckl, and Armbruster,[29] in an investigation of the β decay of ^{101}Nb, have postulated $(\frac{7}{2}, \frac{9}{2})^+$ states at 443 and 317 keV and an isomeric state at 44 keV with $J^\pi=\frac{5}{2}^+$. As discussed below, the higher states would require $l=4$ transfer and would not have been seen in the present study. The resolution attained in this investigation was sufficient to establish that the lowest excited state observed could not lie as low as 44 keV. Thus, if there is an isomeric state at 44 keV, it is not the state observed here at 57 keV.

No states with $l_n=4$ or 5 were identified in this experiment. However, penetration for $l_n=5$ transfer is so inhibited that even a spectroscopic factor of 0.5 would lead to backward angle yields of only

TABLE III. The sums of $S(d,p)$ for the $s_{1/2}$, $d_{3/2}$, and $d_{5/2}$ subshells for Zr and Mo isotopes. The headings $\sum$ and N are the summed strength and the number of states observed to contribute to this sum, respectively.

Target	Reference	$s_{1/2}$ $\sum$	$s_{1/2}$ N	$d_{3/2}$ $\sum$	$d_{3/2}$ N	$d_{5/2}$ $\sum$	$d_{5/2}$ N
^{90}Zr	a	0.96	2	0.99	8	0.89	1
^{94}Zr	a	1.08	3	1.03	13	0.30	1
^{96}Zr	a	0.98	1	0.9	7	0.00	0
^{92}Mo	b	1.08	6	0.97	5	0.87	1
^{94}Mo	b	0.82	8	0.94	19	0.76	2
^{96}Mo	c	0.81	3	0.6–0.9	5–6	0.42	1
^{98}Mo	b	0.76	7	0.64	7	0.23	2
^{100}Mo	d	0.61	3	0.58	4	···	···

[a] B. L. Cohen and O. V. Chubinsky, Phys. Rev. 131, 2184 (1963).

[b] J. B. Moorhead and R. A. Moyer, Phys. Rev. 184, 1205 (1969).

[c] Reference 1.

[d] Present study.

TABLE IV. The sums of $S_j(d,t)$, divided by $(2j+1)$, for several Mo isotopes. These numbers are a measure of the "fullness" of the j subshell, as opposed to the "emptiness" indicated in Table III. These values are from R. C. Diehl, B. L. Cohen, R. A. Moyer, and L. H. Goldman, Phys. Rev. C 1, 2132 (1970).

Target	$s_{1/2}$	$d_{3/2}$	$d_{5/2}$
^{94}Mo	0.10	0.06	0.24
^{96}Mo	0.18	0.14	0.49
^{100}Mo	0.49	0.32	0.64

$\frac{1}{10}$ of the yield of the 290-keV state. Proton groups for such states could be identified only if they were far from other peaks in the spectrum. For a state with $l_n=4$ and $S=0.5$, the backward angle yields would be $\frac{2}{5}$ of those of the 290-keV state. Such a state would have been identified unless it was part of a doublet, not more than about 10 keV from a stronger proton group, since no significant broadening was seen in any of the ^{101}Mo peaks. There is some evidence that the state at 290 keV may be such a doublet. The curvature in the yield as a function of deuteron energy, when plotted logarithmically as in Fig. 5, is upward only for this group; all other groups have downward curvature. This could be explained by assuming a mixture of $l=0$ and $l=4$ contributions; $l=0$ would dominate at lower energies, but at higher energies the greater slope due to $l=4$ would become significant.

The sum of the spectroscopic factors for $s_{1/2}$ and $d_{3/2}$ strengths are 61 and 58%, respectively, of the sum rule limit if $J=\frac{3}{2}^+$ is assumed for the states at 57, 239, 290, and 480 keV and both subshells are assumed vacant. It is possible that not all of these are $\frac{3}{2}^+$, since $\frac{5}{2}^+$ states below 1 MeV in excitation exist in nuclides with $N=59$, 61, and 63. An $s_{1/2}$ contribution from the state at 898 keV has been included since this state has been previously assigned $J=\frac{1}{2}^+$.[1]

Tables III and IV compare the summed (d,p) strengths for the ^{100}Mo(d,p) reaction to the results obtained using targets of even Z and A near 100. The (d,p) stripping results are given in Table III and the (d,t) pickup results in Table IV.

There is an obvious trend in the behavior of the $d_{5/2}$ strength in both the Zr and Mo isotopes in Table III. This strength reflects the fraction of holes remaining in the j subshell of the target nucleus. For both, the $N=50$ isotopes have $d_{5/2}$ strength approaching unity, but this strength decreases quickly and monotonically with increasing N. A value on the order of 0.1 or less may be reasonably expected in ^{100}Mo. Hence our assumption that the observed $l=2$ transitions are likely to be to $\frac{3}{2}^+$ states, rather than to $\frac{5}{2}^+$, appears to be justified.

Table III also shows that the $d_{3/2}$ and $s_{1/2}$ strengths vary more slowly with changing N than does the $d_{5/2}$ strength. In fact, for the Zr isotopes, no significant change is apparent. Our results, for ^{100}Mo, fit the trend in the Mo isotopes quite well.

Table IV lists $S_j(d, t)$, the number of neutrons in the j subshell divided by $(2j+1)$; thus, this gives the *fractional filling* of subshell j. For a particular subshell of a particular target nucleus, this fraction of filling plus the fraction of holes from Table III should sum to unity. This rule can be used to determine if significant strength has been missed in either the (d, p) or (d, t) studies. As seen in Tables III and IV, these sums for ^{100}Mo are ≥ 0.64, 1.10, and 0.90, for $d_{5/2}$, $s_{1/2}$, and $d_{3/2}$, respectively. Some $d_{5/2}$ strength has evidently been missed, but most or all of the $s_{1/2}$ and $d_{3/2}$ strengths have been found.

ACKNOWLEDGMENTS

The authors wish to thank R. W. Hurst and R. L. Boudrie for their assistance during the experiment. In addition they are indebted to P. D. Kunz for generously providing the program DWUCK..

---

*Work supported in part by the U. S. Atomic Energy Commission under Contract No. AT(11-1)-1120, and by the University of Kansas General Research Fund.

†Present address: Los Alamos Scientific Laboratory, Los Alamos, New Mexico.

[1]S. A. Hjorth and B. L. Cohen, Phys. Rev. 135, B920 (1964).

[2]W. Booth, S. M. Dalgliesh, K. C. McLean, R. N. Glover, and F. R. Hudson, Phys. Letters 30B, 335 (1969).

[3]C. F. Moore, P. Richard, C. E. Watson, D. Robson, and J. D. Fox, Phys. Rev. 141, 1166 (1966).

[4]K. A. Ter-Martirosian, Zh. Eksperim. i Teor. Fiz. 29, 713 (1955) [transl.: Soviet Phys.–JETP 2, 620 (1956)].

[5]L. C. Biedenharn, K. Boyer, and M. Goldstein, Phys. Rev. 104, 383 (1956).

[6]R. H. Lemmer, Nucl. Phys. 39, 680 (1962).

[7]A. Dar, A. de-Shalit, and A. S. Reiner, Phys. Rev. 131, 1732 (1963).

[8]F. B. Morinigo, Nucl. Phys. 62, 373 (1965).

[9]L. J. B. Goldfarb, Nucl. Phys. 72, 537 (1965).

[10]W. R. Smith, Nucl. Phys. 72, 593 (1965).

[11]L. J. B. Goldfarb and K. K. Wong, Nucl. Phys. A90, 361 (1967).

[12]M. Dost and W. R. Hering, Phys. Letters 19, 488 (1965); *ibid.* 26B, 443 (1968); Nucl. Phys. A111, 561 (1968).

[13]M. Posner, Phys. Rev. 158, 1018 (1967).

[14]T. Tamaya *et al.*, Nucl. Phys. A126, 449 (1969).

[15]E. B. Dally, J. B. Nelson, and W. R. Smith, Phys. Rev. 152, 1072 (1966).

[16]C. E. Brient, E. L. Hudspeth, E. M. Bernstein, and W. R. Smith, Phys. Rev. 148, 1221 (1966).

[17]R. H. Stokes, Phys. Rev. 121, 613 (1961).

[18]W. D. Barfield, B. M. Bacon, and L. C. Biedenharn, Phys. Rev. 125, 964 (1962).

[19]M. Dost and W. R. Hering, Z. Naturforsch. 21a, 1015 (1966).

[20]J. R. Erskine, W. W. Buechner, and H. A. Enge, Phys. Rev. 128, 720 (1962).

[21]Microfoils, Inc., Argonne, Illinois.

[22]H. M. Kuan *et al.*, University of Kansas Nuclear Structure Laboratory, AEC Technical Report No. COO-1120-88, 1969 (unpublished).

[23]H. M. Kuan *et al.*, University of Kansas Nuclear Structure Laboratory, AEC Technical Report No. COO-1120-117, 1970 (unpublished).

[24]C. Maples, G. W. Goth, and J. Cerny, Lawrence Radiation Laboratory Report No. UCRL-16964, 1967 (unpublished).

[25]P. D. Kunz, University of Colorado, AEC Technical Report No. COO-535-606, 1969 (unpublished).

[26]P. D. Kunz, University of Colorado, AEC Technical Report No. COO-535-613, 1969 (unpublished).

[27]C. M. Perey and F. G. Perey, Phys. Rev. 132, 755 (1963).

[28]F. G. Perey, Phys. Rev. 131, 745 (1963).

[29]J. Eidens, E. Roeckl, and P. Armbruster, Nucl. Phys. A141, 289 (1970).